

Investigation of mode identifiability of a cable-stayed bridge: comparison from ambient vibration responses and from typhoon-induced dynamic responses

Y.Q. Ni^{*}, Y.W. Wang^a and Y.X. Xia^b

*Department of Civil and Environmental Engineering, The Hong Kong Polytechnic University,
Hung Hom, Kowloon, Hong Kong*

(Received October 20, 2014, Revised January 14, 2015, Accepted January 18, 2015)

Abstract. Modal identification of civil engineering structures based on ambient vibration measurement has been widely investigated in the past decades, and a variety of output-only operational modal identification methods have been proposed. However, vibration modes, even fundamental low-order modes, are not always identifiable for large-scale structures under ambient vibration excitation. The identifiability of vibration modes, deficiency in modal identification, and criteria to evaluate robustness of the identified modes when applying output-only modal identification techniques to ambient vibration responses were scarcely studied. In this study, the mode identifiability of the cable-stayed Ting Kau Bridge using ambient vibration measurements and the influence of the excitation intensity on the deficiency and robustness in modal identification are investigated with long-term monitoring data of acceleration responses acquired from the bridge under different excitation conditions. It is observed that a few low-order modes, including the second global mode, are not identifiable by common output-only modal identification algorithms under normal ambient excitations due to traffic and monsoon. The deficient modes can be activated and identified only when the excitation intensity attains a certain level (e.g., during strong typhoons). The reason why a few low-order modes fail to be reliably identified under weak ambient vibration excitations and the relation between the mode identifiability and the excitation intensity are addressed through comparing the frequency-domain responses under normal ambient vibration excitations and under typhoon excitations and analyzing the wind speeds corresponding to different response data samples used in modal identification. The threshold value of wind speed (generalized excitation intensity) that makes the deficient modes identifiable is determined.

Keywords: operational modal identification; mode identifiability; cable-stayed bridge; ambient vibration response; typhoon-induced dynamic response; excitation intensity

1. Introduction

The structural modal properties (including frequencies, damping ratios and modal shapes) are commonly used for dynamic analysis, updating of finite-element models, structural damage

^{*}Corresponding author, Professor, E-mail: ceyqni@polyu.edu.hk

^a Ph.D. Student, E-mail: yw.wang@connect.polyu.hk

^b Ph.D. Student, E-mail: yunxia.xia@connect.polyu.hk

identification and so on. For bridge structures, full-scale vibration test is considered as one of the most reliable experimental methods to assess the actual dynamic properties (Ko *et al.* 2002). There are two commonly used techniques for vibration test of a bridge, namely, forced vibration test and ambient vibration test. In the forced vibration test, the structure is excited by artificial means such as large inertial shakers. Contrarily, the ambient vibration test utilizes natural excitations such as wind and traffic. Because natural excitations have the advantages of low cost, broadband excitation, and no interruption to traffic operation, the ambient vibration test is considered as the most convenient technique and widely used to large-scale civil engineering structures. During the past decades, this technique has been successfully applied to a number of large-scale bridges, such as Vincent Thomas suspension bridge (Abdel-Ghaffar and Housner 1978), Golden Gate suspension bridge (Abdel-Ghaffar and Scanlan 1985), Vasco da Gama Bridge (Cunha *et al.* 2001), Tsing Ma Bridge (Chan *et al.* 2004), International Gvadiana cable-stayed bridge (Magalhães *et al.* 2007), Hakucho suspension bridge (Siringoringo and Fujino 2008), Infante D. Henrique Bridge (Magalhães *et al.* 2008), Gi-Lu cable-stayed bridge (Weng *et al.* 2008), New Carquinez Bridge (Nayeri *et al.* 2009), and Humber Bridge (Brownjohn *et al.* 1994, 2010). The results in general provide reliable and accurate estimates of natural frequencies and modal shapes, despite relatively small amplitudes of structural response.

A variety of output-only operational modal identification methods, by which the modal parameters of a structure can be evaluated from output-only measurements, have been proposed in the past few decades. The output-only modal identification methods can be classified into two main groups, namely, frequency domain methods and time domain methods (Peeters and De Roeck 2001). The major frequency domain methods include the peak picking method (PP) (Bendat and Piersol 1986), the frequency domain decomposition (FDD) (Brincker *et al.* 2001), and the enhanced frequency domain decomposition (EFDD) (Gade *et al.* 2005, Jacobsen *et al.* 2006). The time domain methods include the random decrement technique (RDT) (Ibrahim 1977, Asmussen 1997, Vandiver *et al.* 1982), the natural excitation technique (NExT) (James *et al.* 1995, Barney and Carne 1999), the eigensystem realization algorithm (ERA) (Juang and Pappa 1985, Peterson 1995), the data-driven and covariance-driven stochastic subspace identification (SSI) techniques (Van Overschee and De Moor 1993, Peeters and De Roeck 1999, Peeters and De Roeck 2001, Chen and Huang 2012, Loh *et al.* 2012, Liu *et al.* 2013), and the autoregressive moving average model (ARMA) technique (Pi and Mickleborough 1989, Andersen 1997) among others.

In the meanwhile, it is found that for large-scale structures such as cable-supported bridges, the identification results of modal shape (modal vector) for a particular mode may be significantly different when using ambient vibration responses acquired at different time slots. The identified modal shapes (modal vectors) for a specific mode may all not be the true one, or some of them are representative of the true one while the others are not. Such identification results may result in false-positive damage detection when the ambient vibration responses acquired by an on-line structural health monitoring (SHM) system are used for autonomous modal identification and the identified modal shapes (modal vectors) are utilized for structural damage detection. As a result, it is highly desirable to judge the fidelity of the identified modal shapes (modal vectors) before utilizing them in vibration-based damage detection. While no theoretical criterion is currently available, one is interested in the following question: under what excitation intensity, the identified modes from ambient vibration responses are robust? Making use of the long-term monitoring data of ambient vibration (acceleration) responses acquired from the instrumented Ting Kau cable-stayed bridge under different natural (wind) excitation conditions, the present study firstly recognizes the deficient modes which are unable to be reliably identified from ambient vibration

responses under weak wind conditions. The influence of the excitation intensity on the deficiency and robustness in modal identification is then investigated by using the structural vibration response data acquired during various typhoon events. Finally, the relationship between the mode identifiability and the wind speed (generalized excitation intensity) is figured out to obtain the threshold value of wind speed that ensures a robust identification of modal shapes.

2. Ting Kau Bridge and layout of accelerometers

The Ting Kau Bridge (TKB) is a three-tower cable-stayed bridge with two main spans of 448 m and 475 m respectively, and two side spans of 127 m each (Bergermann and Schlaich 1996). The bridge deck is separated into two carriageways with a width of 18.8 m each, between them being three slender single-leg towers with heights of 170 m, 194 m, and 158 m, respectively. Each carriageway consists of two longitudinal steel girders along the deck edges with steel crossgirders at 4.5 m intervals, and a concrete slab on top. The two carriageways with a 5.2 m gap, are linked at 13.5 m intervals by connecting crossgirders. The deck is supported by 384 stay cables in four cable planes. A unique feature of the bridge is its arrangement of the three single-leg towers which are strengthened by longitudinal and transverse stabilizing cables. Eight longitudinal stabilizing cables with lengths up to 465 m are used to diagonally connect the top of the central tower to the side towers, while 64 transverse stabilizing cables are used to strengthen the three towers in the lateral direction.

As part of a long-term SHM system devised by the Hong Kong SAR Government Highways Department, more than 230 sensors have been permanently installed on the TKB after completing the bridge construction in 1999 (Wong 2004, Ko and Ni 2005). The sensors deployed on the bridge include accelerometers, strain gauges, displacement transducers, anemometers, temperature sensors, GPS, and weigh-in-motion sensors (Wong 2007, Ni *et al.* 2011). 24 uni-axial accelerometers, 20 bi-axial accelerometers and 1 tri-axial accelerometer (totally 67 accelerometer channels) are permanently installed at the deck of the two main spans and two side spans, the longitudinal stabilizing cables, the top of the three towers, and the base of the central tower to monitor the dynamic response of the bridge. In the present study, only the data acquired by the accelerometers deployed at the deck are considered.

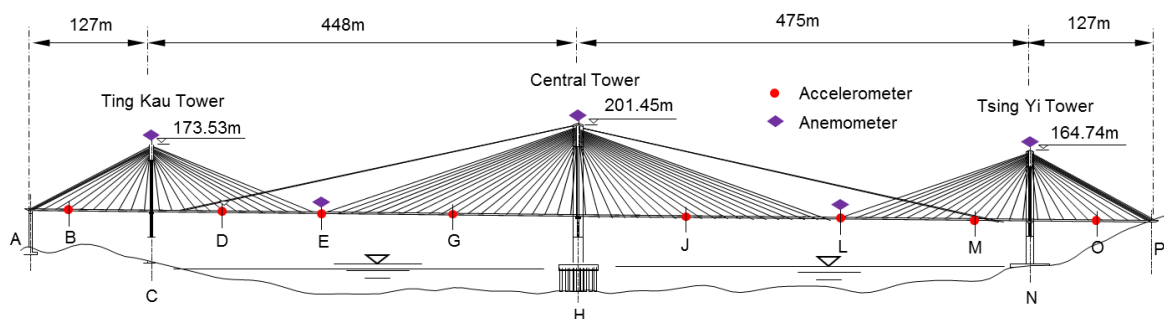


Fig. 1 Ting Kau Bridge (TKB) and layout of accelerometers on bridge deck

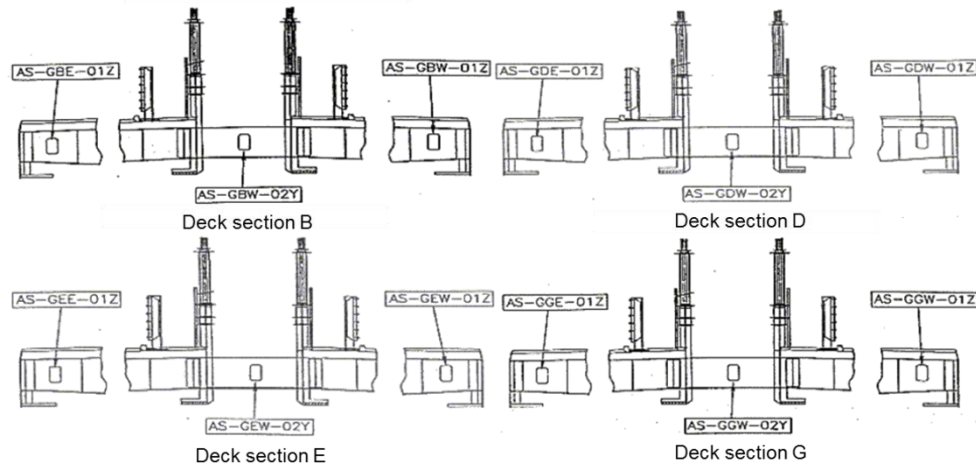


Fig. 2 Deployment of accelerometers on four deck sections

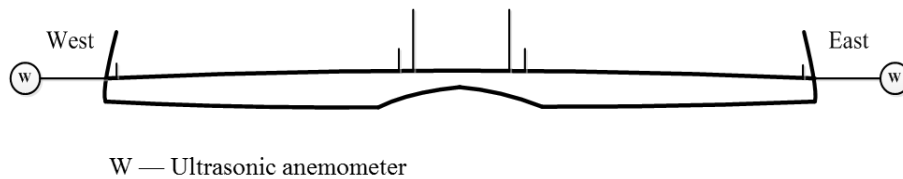


Fig. 3 Deployment of anemometers on deck section

The layout of the accelerometers at eight deck sections on the TKB is shown in Fig. 1. In each section, two accelerometers were installed on the east side and the west side of the longitudinal steel girders respectively to measure the vertical acceleration and one accelerometer was installed on the central crossgirder to measure the transverse acceleration. Fig. 2 illustrates the deployment of accelerometers on four deck sections of the TKB. The sampling frequency was 25.6 Hz. A total of 7 anemometers were installed at the top of the three towers and two main spans (refer to Fig. 1). At each of the two main spans (sections E and L), ultrasonic anemometers were installed on the east and west sides of the deck, respectively, as shown in Fig. 3. The sampling frequency of the anemometers was 2.56 Hz.

3. Mode identifiability under weak wind excitations

The data obtained from the 24 accelerometers deployed on the bridge deck are used to identify modal frequencies and modal shapes (modal vectors) of the bridge. Six sets of data samples, each lasting for one hour, are selected. They are from different months and under distinct wind speeds.

Table 1 Six data samples selected under weak wind conditions

Sample	Time duration	Mean hourly wind speed (m/s)	Mean hourly wind direction* (°)
Sample 1	15:00-16:00, 28 Dec 1999	2.00	275
Sample 2	15:00-16:00, 18 Feb 1999	3.40	328
Sample 3	15:00-16:00, 01 Mar 1999	3.34	227
Sample 4	15:00-16:00, 21 Jun 1999	3.41	185
Sample 5	15:00-16:00, 24 Jul 1999	6.17	117
Sample 6	15:00-16:00, 12 Aug 1999	4.20	274

*Note: 0 degree wind direction denotes wind blowing from due north and clockwise direction is positive.

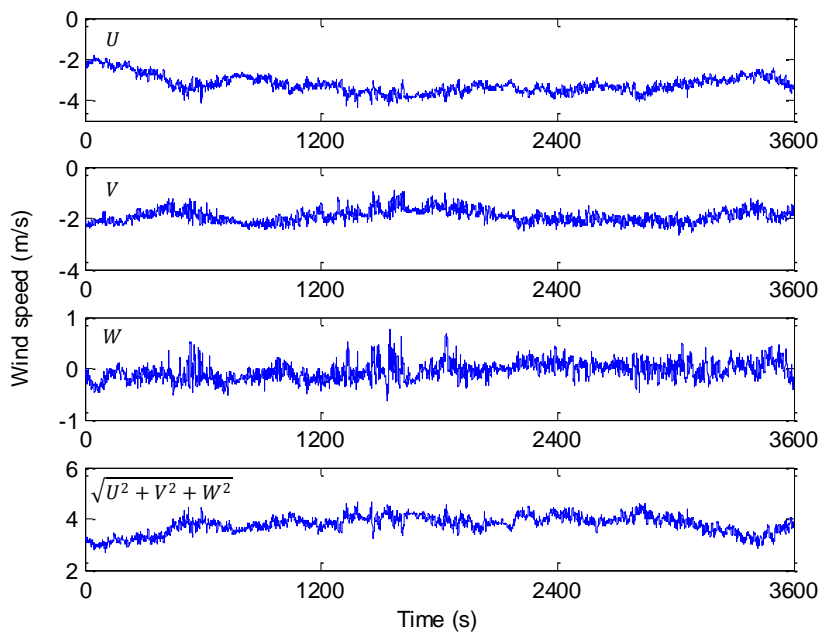


Fig. 4 Wind components of Sample 3 (from the anemometer located on the west side of section E)

Table 1 shows the information about the samples and the associated mean hourly wind speeds and directions. In order to accurately obtain the mean hourly wind speed at the deck level, the data acquired from the anemometers located on the windward side of the deck are used to calculate the mean hourly wind speed because the wind speed on the leeward side is influenced by the bridge deck and that on the windward is real wind speed. The time histories of the U -, V -, W -direction wind speed components for Sample 3 are depicted in Fig. 4 (U is the horizontal direction

perpendicular to the alignment of the bridge deck; V is the horizontal direction parallel to the alignment of the bridge deck; and W is the vertical direction perpendicular to the horizontal plane formed by U - V directions). It can be seen that the mean hourly wind speeds for all the six samples are not large (the maximum one is 6.17 m/s), which are regarded as weak wind conditions (Chiu 2014). Fig. 5 shows the acceleration responses of Sample 6 on sections G and L of the bridge deck. It is clear that the acceleration in the vertical direction is much larger than that in the lateral direction.

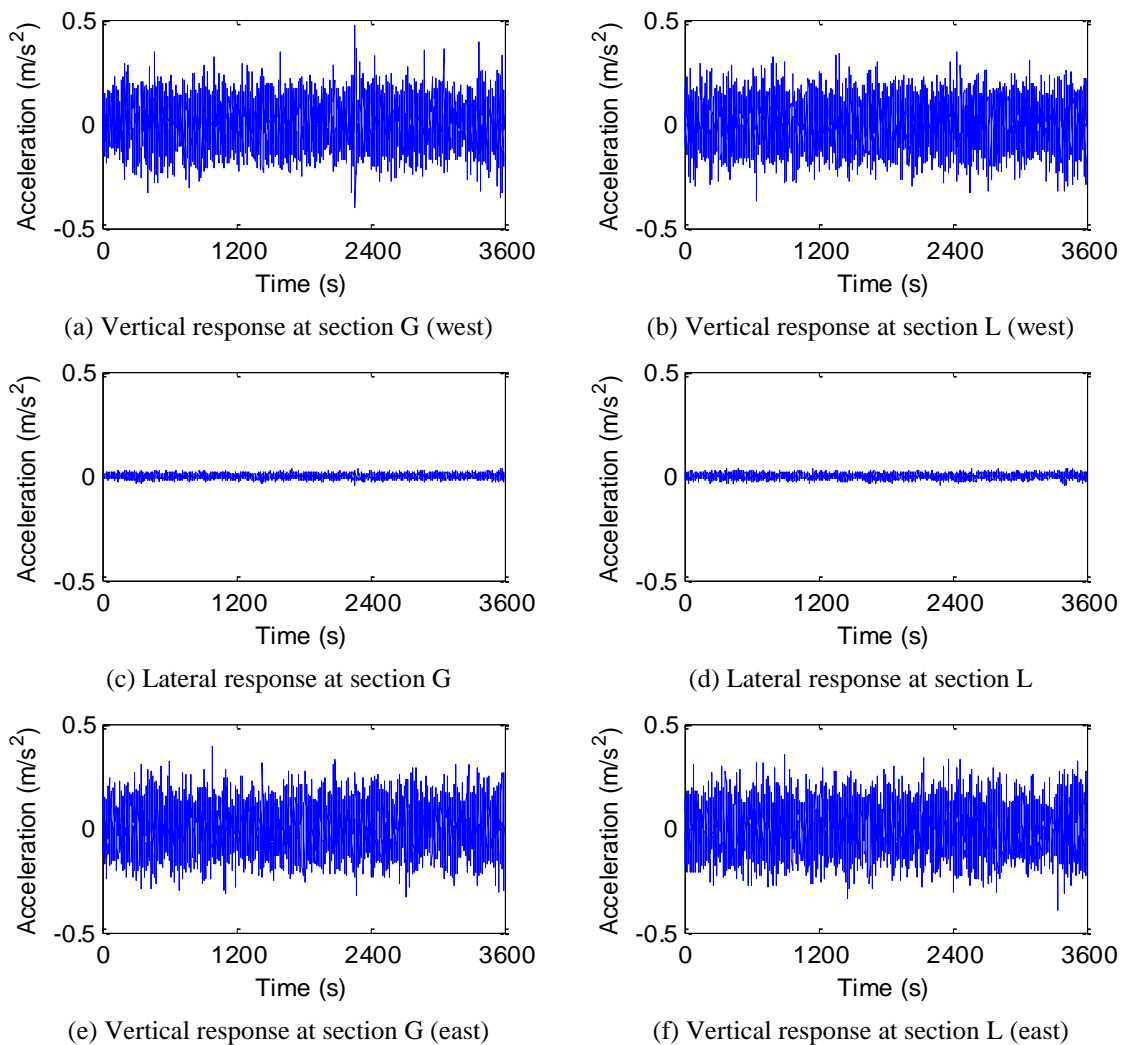


Fig. 5 Time histories of acceleration responses for Sample 6

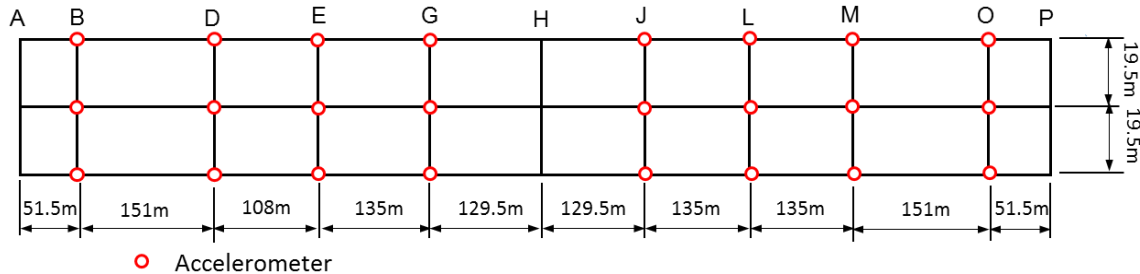


Fig. 6 Geometry configuration of accelerometers on bridge deck

Table 2 Identified modal frequencies of the first ten modes under weak wind conditions

Mode No.	Frequency (Hz)						Description
	S1	S2	S3	S4	S5	S6	
1	0.162	0.162	0.163	0.164	0.163	0.165	Predominantly vertical mode
2	0.226	0.230	0.224	0.229	0.224	0.223	----
3	0.257	0.259	0.259	0.258	0.257	0.260	Predominantly lateral mode
4	0.288	0.290	0.288	0.288	0.285	0.287	Coupled torsional & lateral mode
5	0.300	0.300	0.300	0.300	0.300	0.299	Predominantly vertical mode
6	0.310	0.313	0.311	0.316	0.314	0.320	Coupled torsional & lateral mode
7	0.358	0.358	0.358	0.359	0.357	0.359	Predominantly vertical mode
8	0.373	0.373	0.372	0.373	0.371	0.372	Predominantly vertical mode
9	0.385	0.384	0.383	0.382	0.384	0.383	Predominantly vertical mode
10	0.397	0.398	0.400	0.397	0.393	0.394	Predominantly vertical mode

The data driven stochastic subspace identification (data-driven SSI) technique is considered to be the most powerful class of the known identification techniques for operational modal analysis in the time domain (Brincker and Andersen 2006), and is applied to identify the modal frequencies and modal shapes of the TKB from ambient vibration responses in the present study. The data-driven SSI technique works directly with the recorded time domain signals. It identifies state space models from the output data by applying robust numerical techniques such as QR factorization, SVD (singular value decomposition) and least squares. Roughly, the QR results in significant data reduction while SVD is used to reject the noise assumed to be represented by the higher singular values. Once the state space model has been formulated, it is straightforward to

determine the modal parameters by eigenvalue decomposition: natural frequencies, damping ratios and modal shapes. There exist three main algorithms for weighting the data matrices before the application of SVD: Canonical Variate Analysis (CVA), Principal Components (PC), and Unweighted Principal Components (UPC). In the present study, the data-driven SSI associated with UPC is utilized. Fig. 6 shows the geometry configuration of accelerometer deployment on the TKB deck, on which the identified modal shapes (modal vectors) will be plotted. The first ten modes are identified and classified. The identified frequencies of the first ten modes are given in Table 2, which are all within the range of 0.15 to 0.40 Hz. The results of modal frequency for each mode identified from the different data samples are consistent with each other.

Fig. 7 to Fig. 11 show the modal shapes (modal vectors) of the first, second, third, fifth, and eighth modes identified from the six sets of data samples. The lines with square and triangle symbols denote the modal responses from the vertical accelerometers, while the line with diamond symbols indicates the modal responses from the transverse accelerometers. It is observed that from the six sets of data samples, the identified modal shapes (modal vectors) of the first ten modes, except the second mode, are in general consistent in each mode. The first, fifth, seventh, eighth, ninth, and tenth modes are predominantly vertical modes, and the fourth and sixth modes are coupled torsional and lateral modes, and only the third mode is a predominantly lateral mode. However, the identified modal shapes (modal vectors) of the second mode are ambiguous and distinct from different data sets. Therefore the second mode is recognized as a deficient mode and further investigation will be made to determine the modal shape of the second mode.

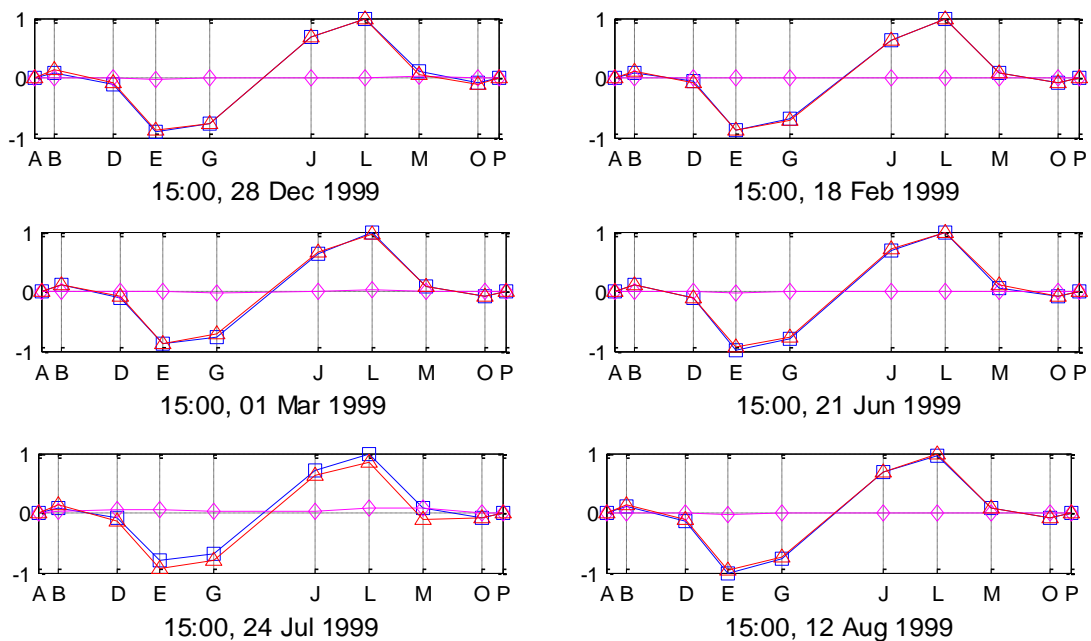


Fig. 7 Identified modal shapes of the 1st mode

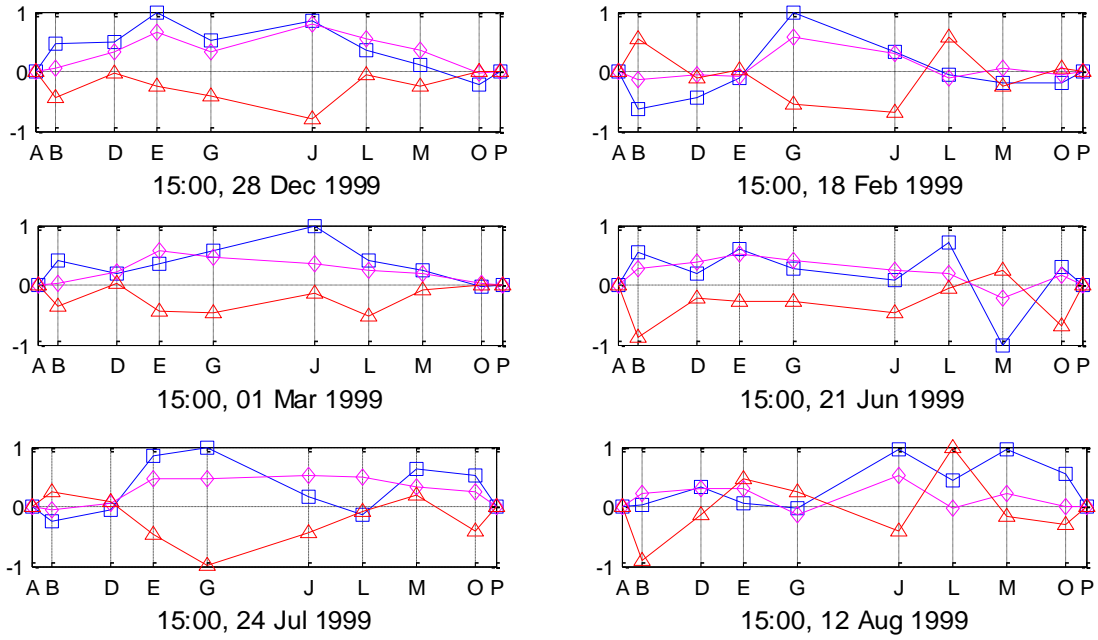


Fig. 8 Identified modal shapes of the 2nd mode

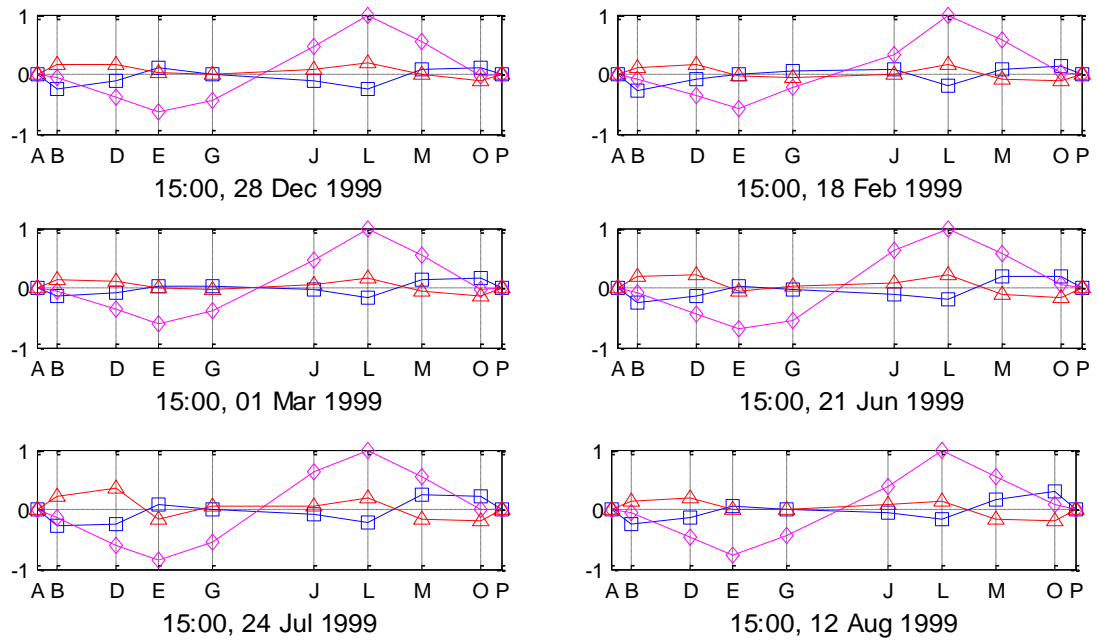


Fig. 9 Identified modal shapes of the 3rd mode

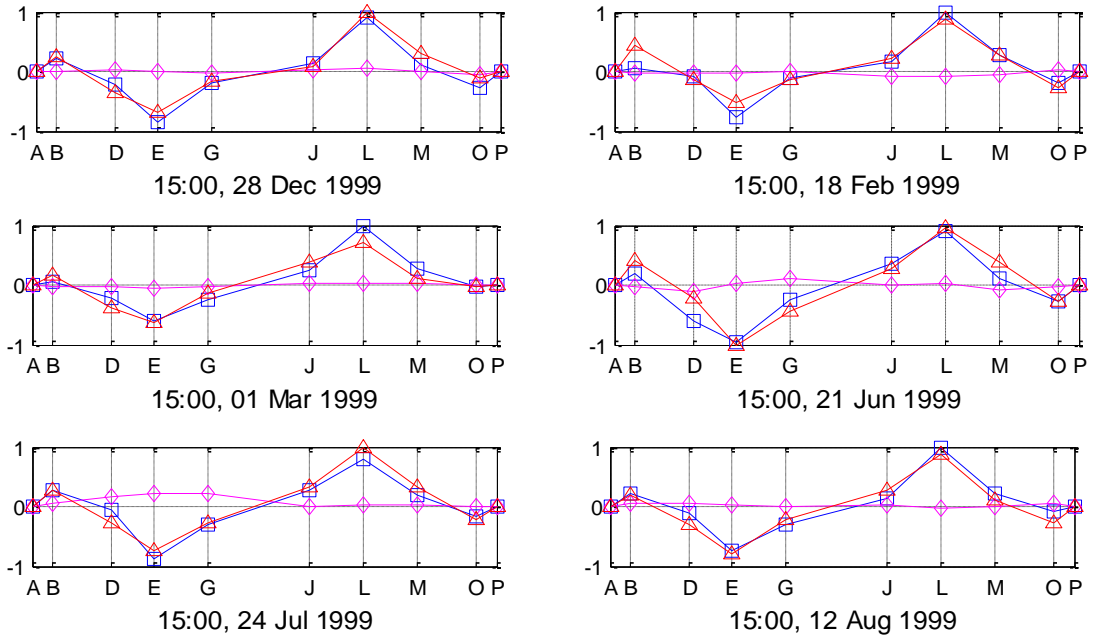


Fig. 10 Identified modal shapes of the 5th mode

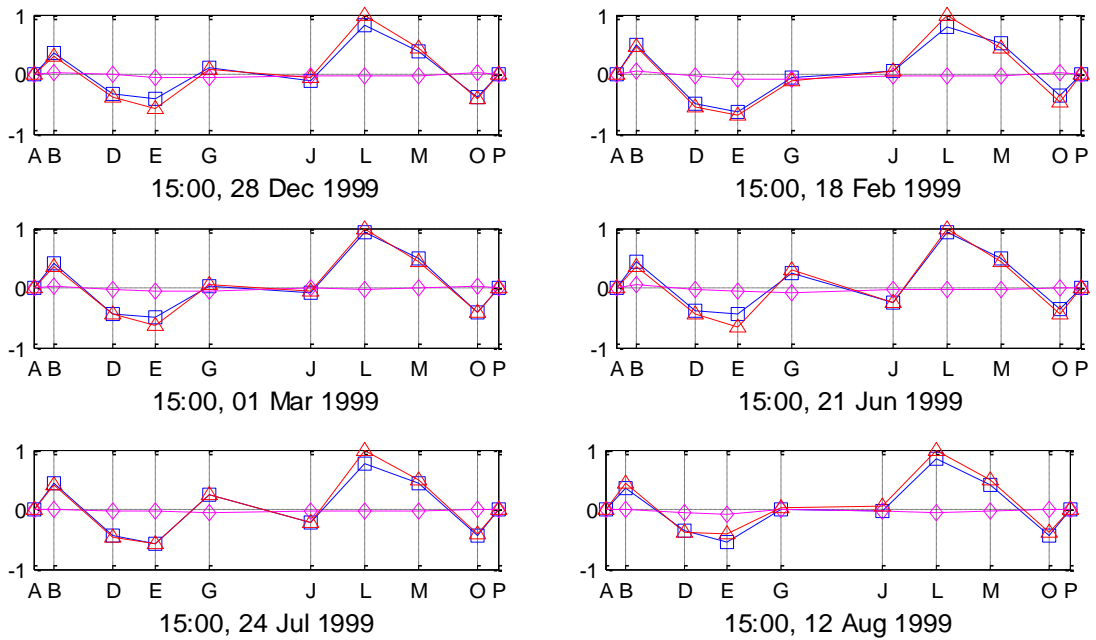


Fig. 11 Identified modal shapes of the 8th mode

4. Mode identifiability under typhoon excitations

It has been shown in the above that the modal shape of the second mode is unidentifiable when using ambient vibration responses under weak wind excitation conditions. It is conjectured that the unidentifiability is due to that the modal energy poured into the second mode under weak wind excitations is not large enough to activate this mode. With this conjecture, the structural vibration response data obtained during strong typhoons are chosen to carry out the modal identification again. According to the record by the Hong Kong Observatory, three typhoons, 'Maggie', 'Sam' and 'York' hit Hong Kong on 7 June, 22 August and 16 September in 1999 (Hong Kong Observatory 2000). All the three typhoons made the hoisting of Typhoon Signal No. 8 or above in Hong Kong. The time histories of the U -, V -, W -direction wind speed components during Typhoon 'York' are depicted in Fig. 12.

Table 3 provides four sets of data samples selected during the typhoons and the associated mean hourly wind speeds and directions. It is seen that the mean hourly wind speed at the bridge deck level is 12.11 m/s, 15.62 m/s, 21.72 m/s, and 15.91 m/s, respectively, which are much higher than those of the previous six sets of data samples. Fig. 13 shows the acceleration responses on sections G and L of the bridge deck during Typhoon 'York' (06:00-07:00). It is interesting to note that the vertical acceleration responses of the bridge deck under the typhoon conditions are less than those under normal conditions (but the lateral acceleration responses of the deck under the typhoon conditions are larger than those under normal conditions). This is because during the strong typhoon periods all vehicles were prohibited to run on the bridge. For this extremely flexible cable-stayed bridge, the traffic-induced vertical vibration is significant.

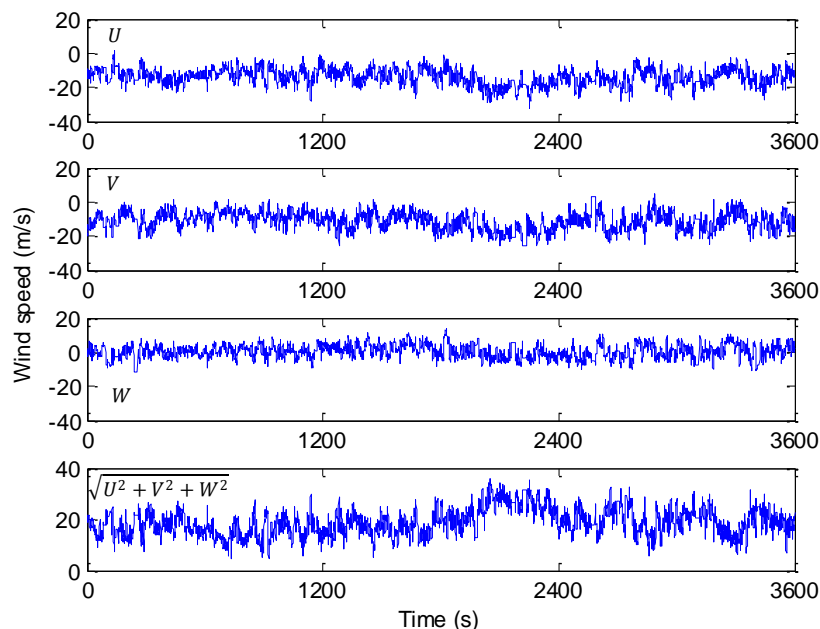


Fig. 12 Wind components during Typhoon York (from the anemometer located on the east side of section L)

Table 3 Four data samples selected under typhoon conditions

Typhoon	Time duration	Mean hourly wind speed (m/s)	Mean hourly wind direction* (°)
Maggie	03:00-04:00, 07 Jun 1999	12.11	324
Sam	02:00-03:00, 23 Aug 1999	15.62	218
York 1	06:00-07:00, 16 Sep 1999	21.72	28
York 2	15:00-16:00, 16 Sep 1999	15.91	181

*Note: 0 degree wind direction denotes wind blowing from due north and clockwise direction is positive.

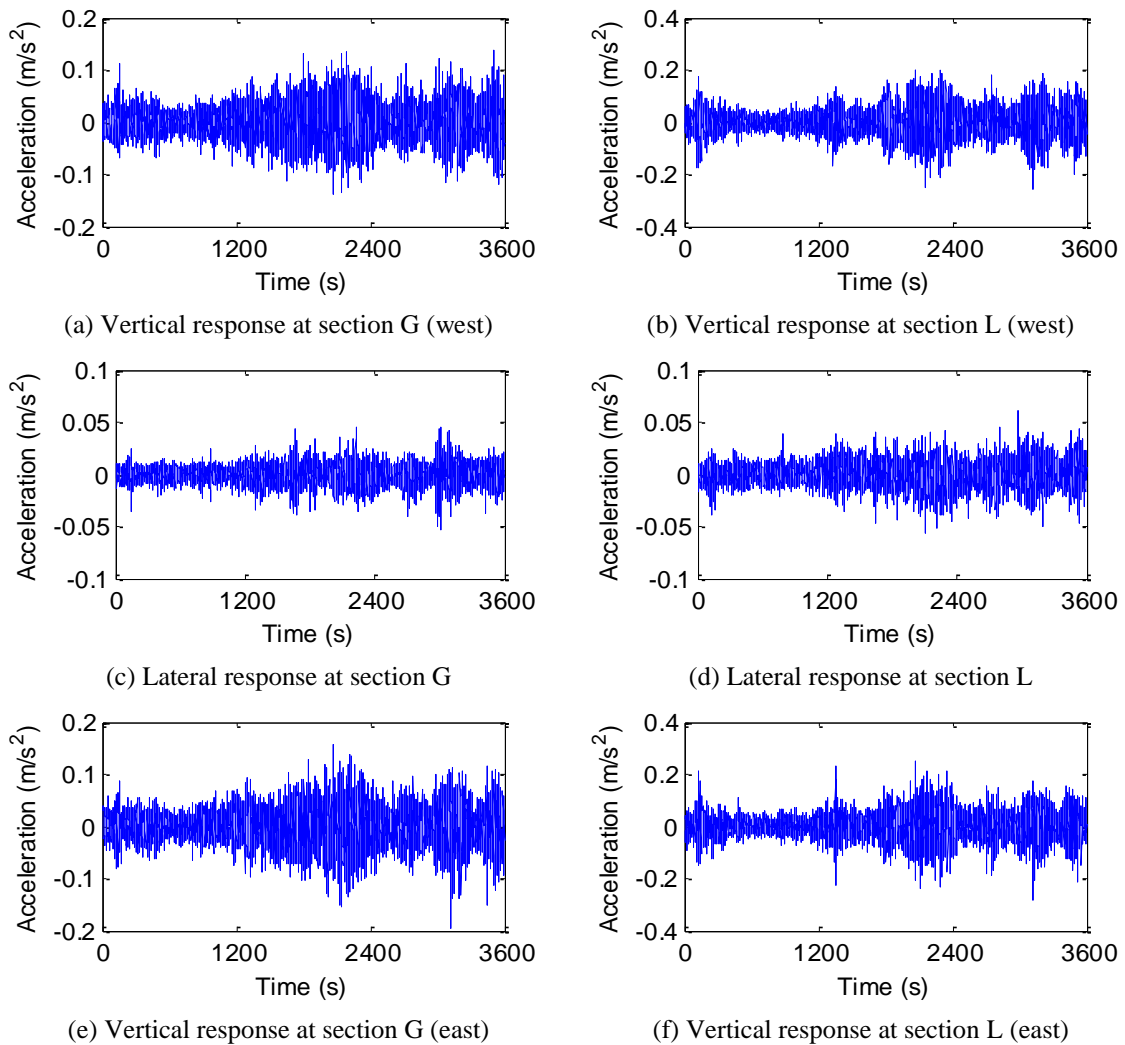


Fig. 13 Time histories of acceleration responses during Typhoon York (06:00-07:00)

The modal identification using the four sets of data samples obtained during strong typhoons is conducted in the same way by applying the data-driven SSI technique. Table 4 shows the identified modal frequencies of the first ten modes. The identified results of modal frequency for each mode from the four data samples are consistent. Fig. 14 provides a comparison of the modal frequencies identified under typhoon conditions with those identified under weak wind conditions. A good agreement is observed. Fig. 15 shows the identified modal shapes (modal vectors) and description of the first ten modes by using the acceleration response data acquired during the typhoon ‘Sam’. By comparing Fig. 15 with Fig. 7 to Fig. 11, it is observed that the modal shapes (modal vectors) identified under typhoon conditions are coincident well with those identified under weak wind conditions, except for the second mode.

Table 4 Identified modal frequencies of the first ten modes under typhoon conditions

Mode No.	Frequency (Hz)				Description
	Maggie	Sam	York 1	York 2	
1	0.165	0.164	0.164	0.166	Predominantly vertical mode
2	0.227	0.227	0.227	0.226	Coupled torsional & lateral mode
3	0.262	0.264	0.258	0.260	Predominantly lateral mode
4	0.290	0.290	0.285	0.288	Coupled torsional & lateral mode
5	0.301	0.298	0.300	0.301	Predominantly vertical mode
6	0.322	0.324	0.319	0.316	Coupled torsional & lateral mode
7	0.361	0.361	0.358	0.357	Predominantly vertical mode
8	0.372	0.372	0.373	0.372	Predominantly vertical mode
9	0.385	0.385	0.384	0.385	Predominantly vertical mode
10	0.395	0.393	0.394	0.393	Predominantly vertical mode

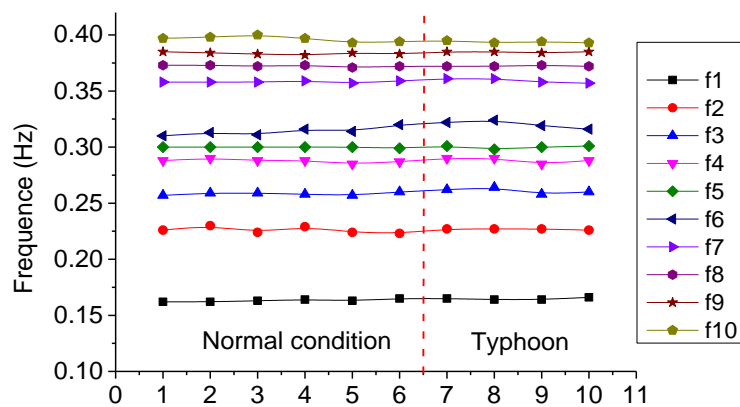


Fig. 14 Identified modal frequencies under weak and strong wind conditions

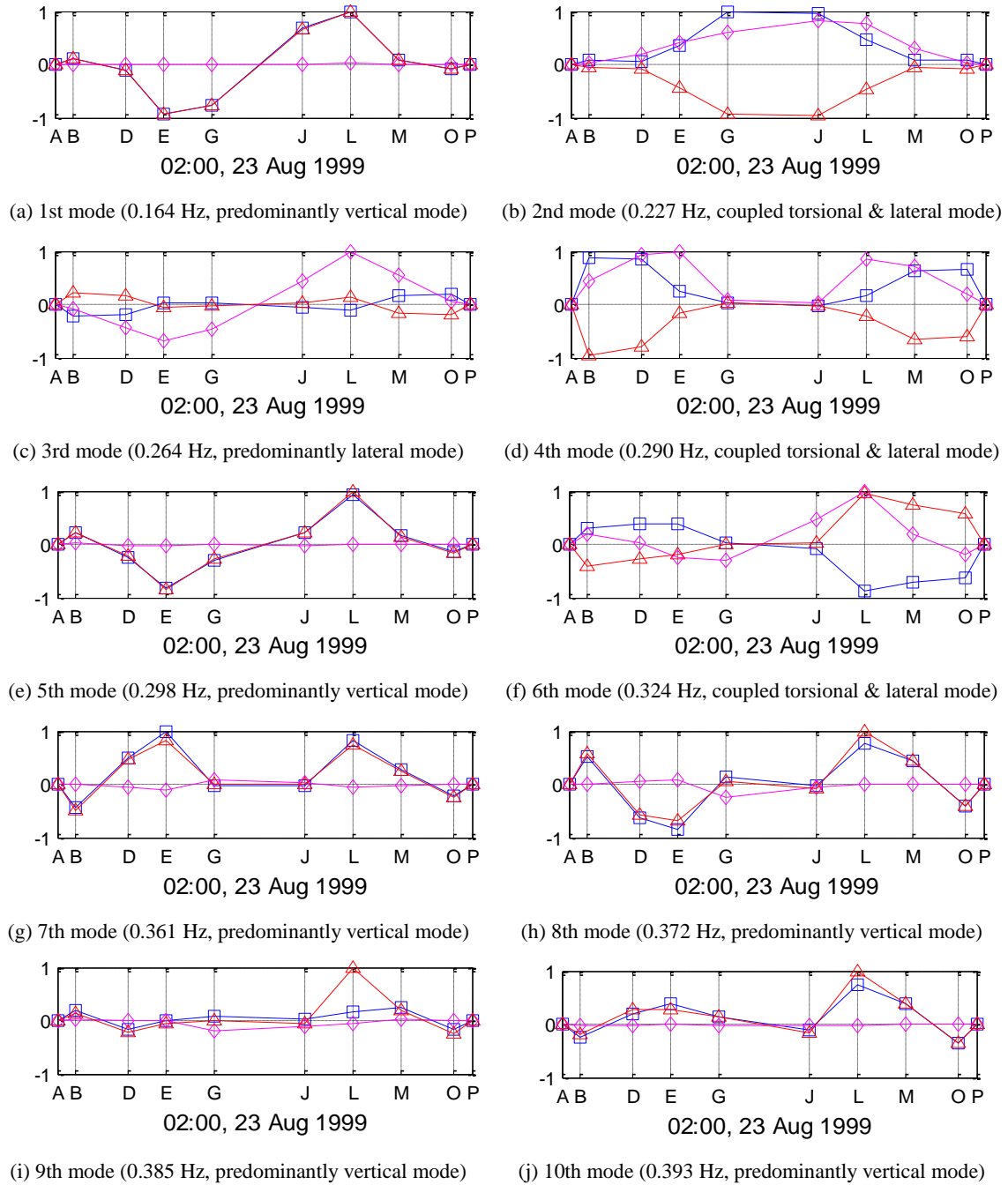


Fig. 15 Identified modal shapes and description of the first ten modes (Typhoon Sam)

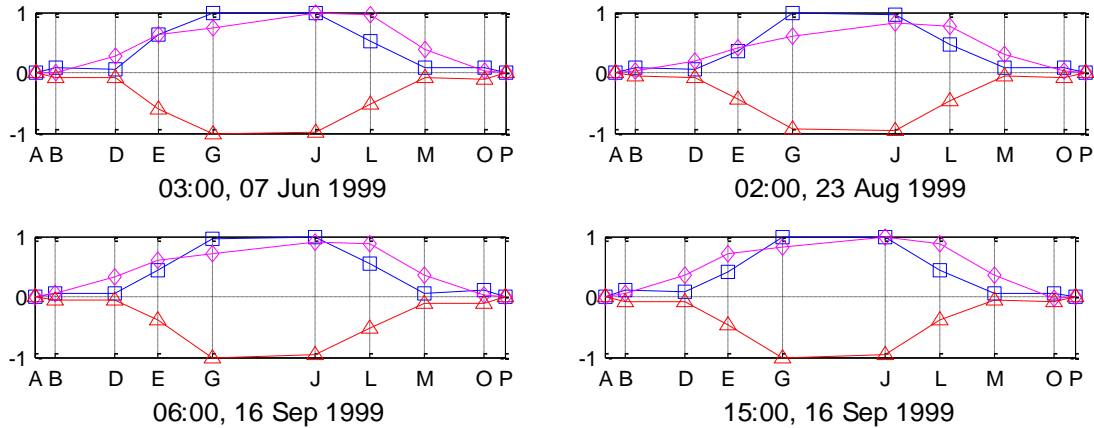


Fig. 16 Identified modal shapes of the 2nd mode

Fig. 16 shows the results of modal shapes of the second mode (a coupled torsional and lateral mode) identified using the four data samples obtained under different typhoon conditions. It is observed that the identified modal shapes are highly consistent with each other, confirming the robustness of the identified modal shapes.

5. Comparison of modal shapes and damping ratios of the second mode under different excitation conditions

To further understand the identified modal shapes of the second mode identified under different excitation conditions, the vertical, lateral and torsional response components are separately extracted for modal analysis: the vertical response component is obtained by averaging the synchronously acquired dynamic responses from the two vertical accelerometers on the east and west sides respectively of the same deck section; the lateral response component is obtained from the lateral accelerometer deployed at the central crossgirder; and the torsional response component is obtained by subtracting the synchronously acquired dynamic responses from the two vertical accelerometers on the east and west sides respectively of the same deck section. Applying the SSI technique, the modal shapes of the bridge deck are identified again by using the three response components under different excitation conditions. The results show that the second mode cannot be identified from the vertical response component (the second mode is irrelevant to the vertical response). Fig. 17 illustrates the modal shapes of the second mode identified under weak wind conditions (cases (a)-(d)) and under typhoon conditions (cases (e)-(h)). The lines with circle symbols denote the modal response from the torsional acceleration, while the lines with diamond symbols indicate the modal response from the lateral acceleration. It is seen that the difference of modal vectors identified from the lateral acceleration under different weak wind conditions is not obvious; however, the modal vectors identified from the torsional acceleration under different weak wind conditions vary greatly. Both the lateral and torsional modal vectors identified under different typhoon conditions are consistent. It is therefore concluded that the modal deficiency of the second mode is mainly resulting from the torsional response.

The identified damping ratios of the deficient mode (second mode) under different excitation conditions are given in Table 5. The damping ratios identified under weak wind conditions are far larger than those identified under typhoon conditions. Because the modal responses of the second mode are not well activated under weak wind conditions, the excessively large damping ratios identified under weak wind conditions are untrue whereas those identified under typhoon conditions have higher fidelity.

Table 5 Identified modal damping ratios of the second mode under different excitations

	Under weak wind conditions						Under typhoon conditions			
Sample	S1	S2	S3	S4	S5	S6	Maggie	Sam	York 1	York 2
Damping ratio (%)	1.70	2.64	2.50	4.46	1.92	2.56	0.67	0.46	0.46	0.65

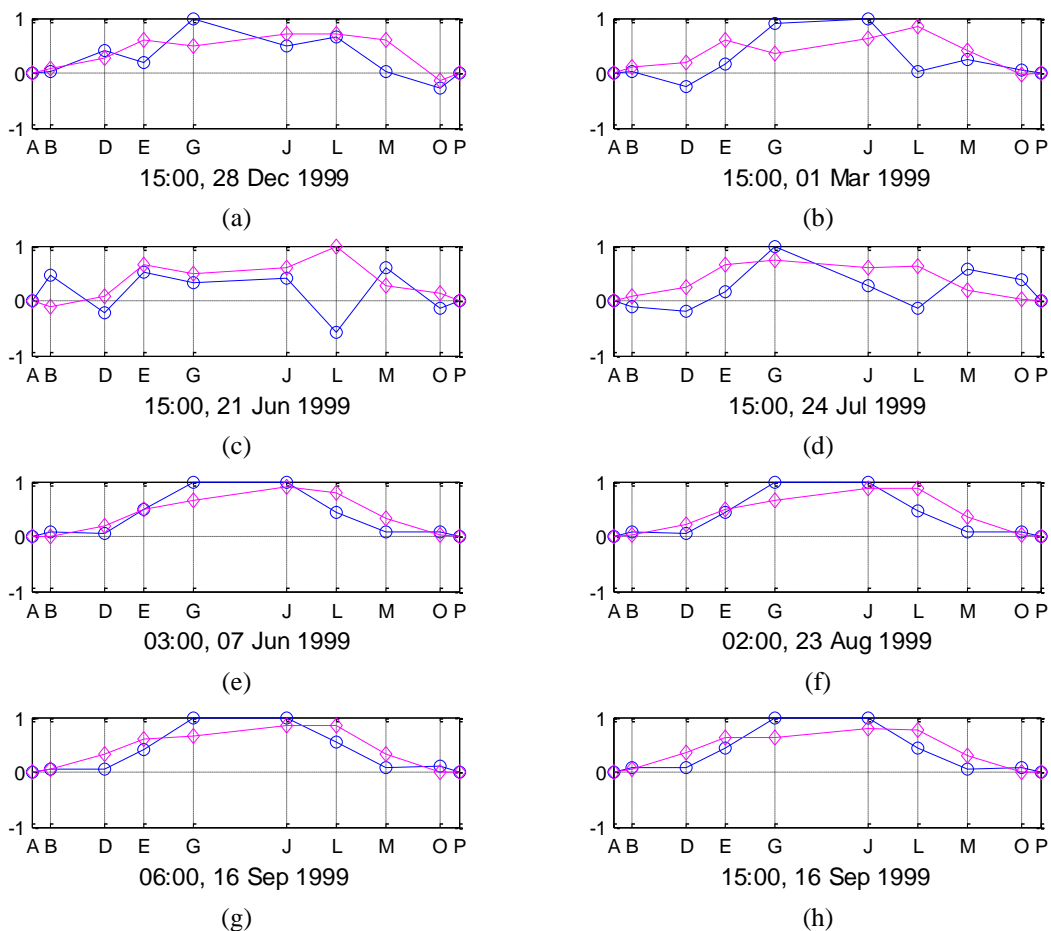


Fig. 17 Identified modal shapes of the 2nd mode under different excitation conditions

6. Influence of excitation intensity on mode identifiability

To understand why a mode can be deficient to accurately identify its modal shape when using ambient vibration responses under weak excitation conditions and to determine the threshold of excitation intensity that ensures a reliable identification of modal shape, spectral analyses are conducted on the wind speed and acceleration response data acquired under both weak and strong wind conditions. Fig. 18 shows the wind spectra under weak wind conditions (Figs. 18(a) and 18(b)) and under typhoon conditions (Figs. 18(c) and 18(d)). It can be seen that the power spectra (in the frequency range between 0.1 and 1.0 Hz) under weak wind conditions are much smaller than those under typhoon conditions, implying that much less excitation energy was generated in the former. Fig. 19 illustrates the auto-spectra of the structural dynamic responses under weak wind conditions (Figs. 19(a) and 19(b)) and under typhoon conditions (Figs. 19(c) and 19(d)). The modal frequency of the second mode is identified to be about 0.227 Hz. It is seen that the modal responses at around 0.227 Hz are very small (almost unidentifiable) under weak wind conditions (Figs. 19(a) and 19(b)). However, the modal responses at around 0.227 Hz are clearly activated under typhoon conditions (Figs. 19(c) and 19(d)), making the modal shape identifiable.

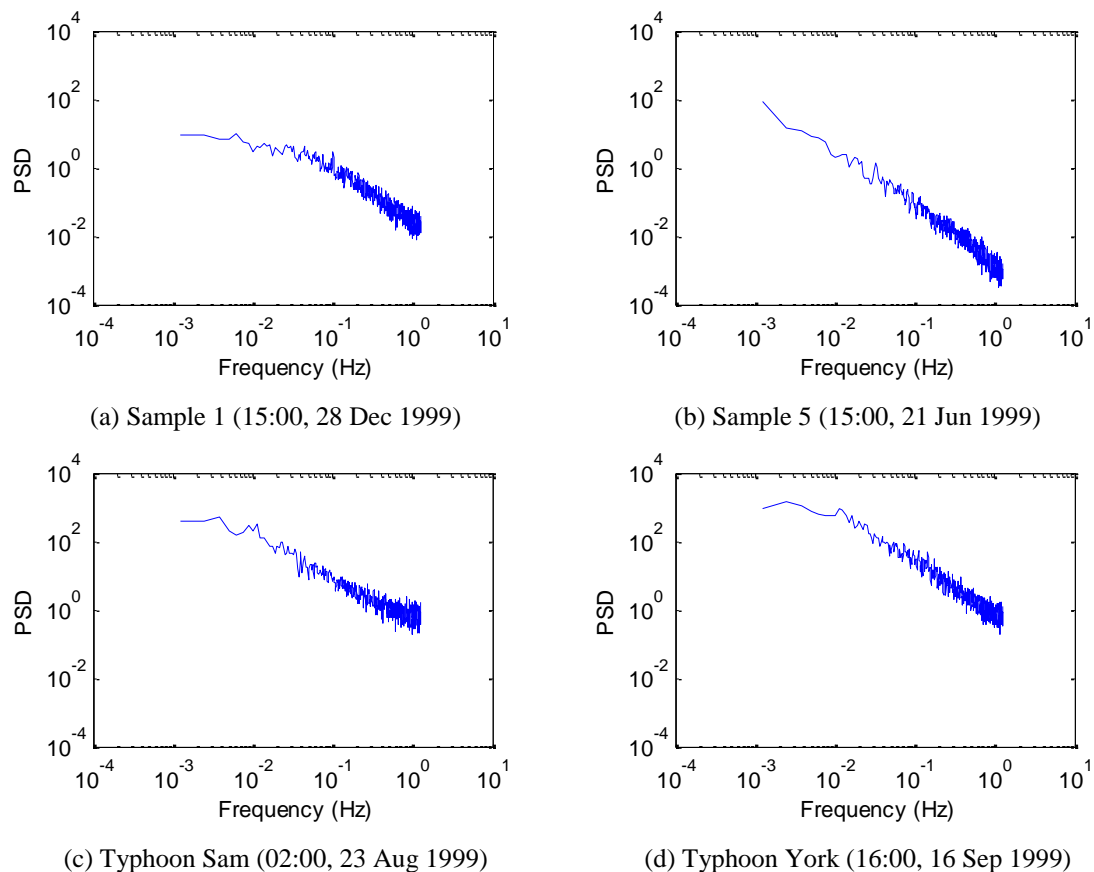


Fig. 18 Comparison of wind spectra under different excitation conditions

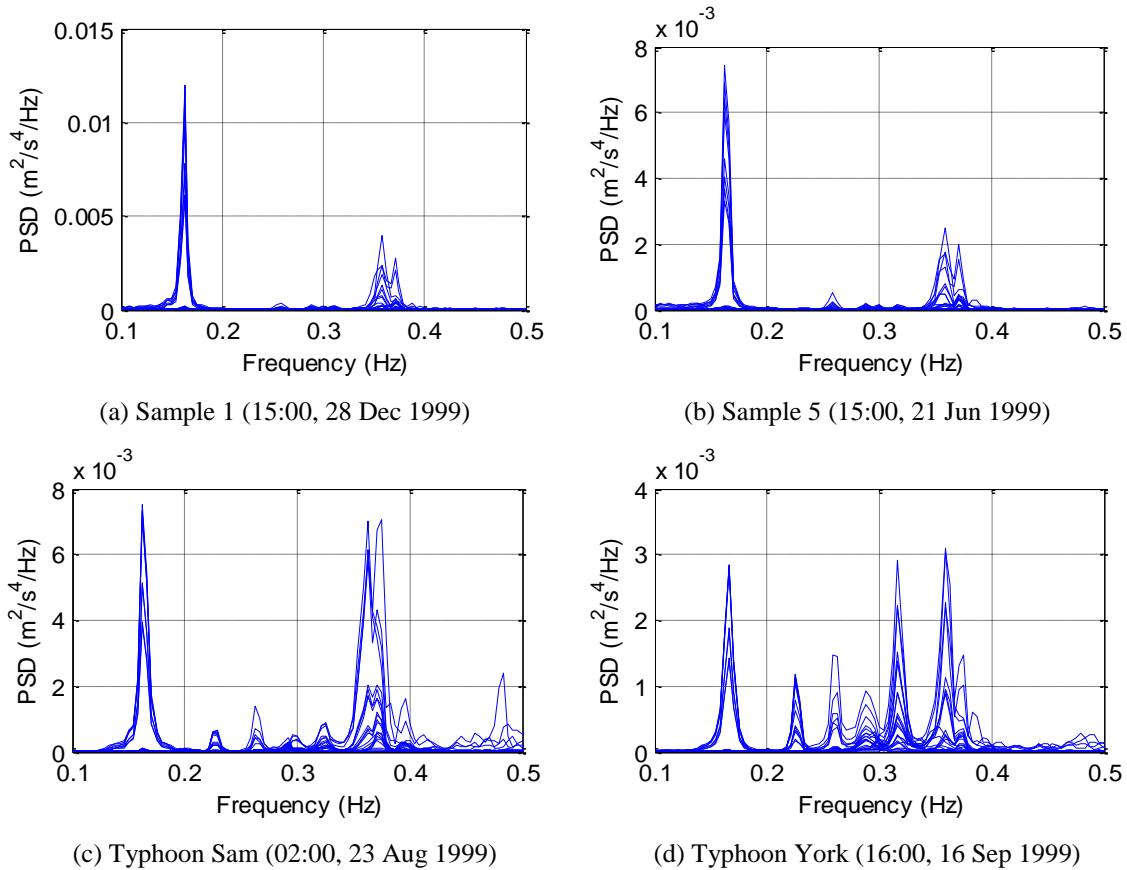


Fig. 19 Comparison of response auto-spectra under different excitation conditions

The amplitudes of power spectral densities (PSD) of the structural responses at the second mode have been obtained for all the 10 data samples (six data samples under weak wind conditions and four data samples under typhoon conditions). The PSD amplitudes and the corresponding mean hourly wind speeds for the 10 data samples are shown in Fig. 20. It is observed that when the mean hourly wind speed is lower than about 7.5 m/s, the PSD amplitude for the second mode is almost not varying with the variation in wind speed; however, when the mean hourly wind speed is higher than about 7.5 m/s, the PSD amplitude for the second mode proportionally increases with the increase of wind speed and this increase is significant. It can be concluded that when the mean hourly wind speed is below about 7.5 m/s, the modal response of the second mode cannot be activated and therefore its modal shape is unidentifiable; when the mean hourly wind speed is higher than about 7.5 m/s, the modal response of the second mode is activated (the evidence is that its PSD amplitude proportionally increases with increasing wind speed) and its modal shape is identifiable. Therefore, the threshold of the generalized excitation intensity (wind speed) which ensures a reliable identification of modal shape (modal vector) for the second mode (deficient mode) is around 7.5 m/s. When an autonomous output-only modal identification code is

incorporated in an on-line SHM system to continually identify modal parameters (inclusive of the second mode) for vibration-based structural damage detection, only the results of the identified modal shapes when the mean hourly wind speed exceeds 7.5 m/s should be used. Fig. 21 shows the PSD amplitudes and the corresponding mean hourly wind directions for the 10 data samples, no relation between them being observed.

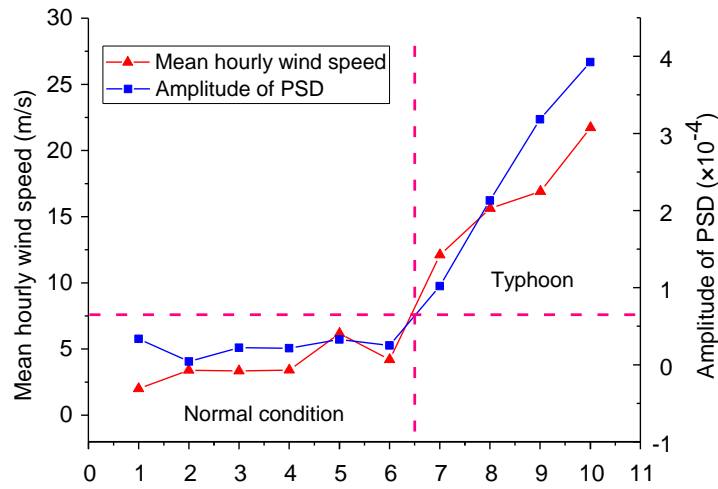


Fig. 20 Variation of mean hourly wind speed and PSD amplitude for the 2nd mode

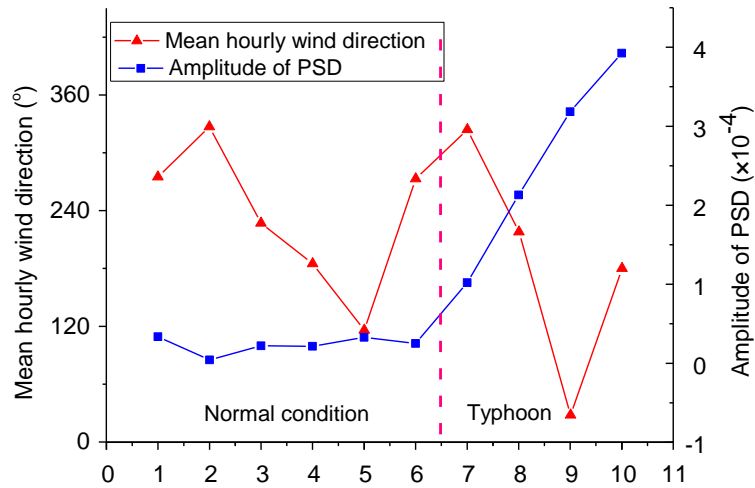


Fig. 21 Variation of mean hourly wind direction and PSD amplitude for the 2nd mode

7. Conclusions

This paper addresses the mode identifiability of large-scale structures using output-only modal identification techniques. By using the dynamic response monitoring data of the instrumented Ting Kau Bridge (TKB) acquired under different wind excitation conditions, the deficient mode which is identifiable under weak wind conditions is first recognized, followed by the identification of modal shape of the deficient mode using the acceleration response data obtained under typhoon conditions. It is revealed that: (i) when the ambient excitation (wind speed) is lower than a certain value, the modal responses at the deficient mode(s) are very small and almost independent of the excitation intensity (not varying with wind speed), thus making the modal shapes of the deficient mode(s) unidentifiable; (ii) when the ambient excitation (wind speed) is higher than a certain value, the modal responses at the deficient mode(s) significantly increase with the increase of the excitation intensity (wind speed), thereby making the modal shapes identifiable; (iii) Once the excitation intensity (wind speed) exceeds a certain value, the identified modal shapes using the structural dynamic responses obtained under different typhoon conditions are consistent and reliable; and (iv) a threshold value of the generalized excitation intensity (wind speed) that ensures a reliable identification of modal shapes can be obtained.

Acknowledgments

The work described in this paper was supported by a grant from the Research Grants Council of the Hong Kong Special Administrative Region, China (Project No. PolyU 5224/13E). The writers also wish to thank the Hong Kong SAR Government Highways Department for providing the long-term structural health monitoring data of the Ting Kau Bridge.

References

- Abdel-Ghaffar, A.M. and Housner, G.W. (1978), "Ambient vibration tests of suspension bridge", *J. Eng. Mech. - ASCE*, **104**(5), 983-999.
- Abdel-Ghaffar, A.M. and Scanlan, R.H. (1985), "Ambient vibration studies of Golden Gate Bridge: I. suspended structure", *J. Eng. Mech. - ASCE*, **111**(4), 463-482.
- Andersen, P. (1997), *Identification of civil engineering structures using vector ARMA models*, PhD Thesis, Department of Building Technology and Structural Engineering, Aalborg University, Aalborg, Denmark.
- Asmussen, J.C. (1997), *Modal analysis based on the random decrement technique*, PhD Thesis, Department of Building Technology and Structural Engineering, Aalborg University, Aalborg, Denmark.
- Barney, P. and Carne, T. (1999), "Modal parameter extraction using natural excitation response data", *Proceedings of the 17th International Modal Analysis Conference*, Orlando, Florida, USA.
- Bendat, J.S. and Piersol, A.G. (1986), *Random Data: Analysis and Measurement Procedures*, John Wiley & Sons, New York, USA.
- Bergermann, R. and Schlaich, M. (1996), "Ting Kau Bridge, Hong Kong", *Struct. Eng. Int.*, **6**(3), 152-154.
- Brincker, R. and Andersen, P. (2006), "Understanding stochastic subspace identification", *Proceedings of the 24th International Modal Analysis Conference*, St. Louis, Missouri, USA.
- Brincker, R., Zhang, L. and Andersen, P. (2001), "Modal identification of output-only systems using frequency domain decomposition", *Smart Mater. Struct.*, **10**(3), 441-445.
- Brownjohn, J.M.W., Boccione, M., Curami, A., Falco, M. and Zasso, A. (1994), "Humber Bridge full-scale measurement campaigns 1990-1991", *J. Wind Eng. Ind. Aerod.*, **52**, 185-218.

- Brownjohn, J.M.W., Magalhaes, F., Caetano, E. and Cunha, A. (2010), "Ambient vibration re-testing and operational modal analysis of the Humber Bridge", *Eng. Struct.*, **32**(8), 2003-2018.
- Chan, T.H., Li, Z.X. and Ko, J.M. (2004), "Evaluation of typhoon induced fatigue damage using health monitoring data for the Tsing Ma Bridge", *Struct. Eng. Mech.*, **17**(5), 655-670.
- Chen, H.P. and Huang, T.L. (2012), "Updating finite element model using dynamic perturbation method and regularization algorithm", *Smart Struct. Syst.*, **10**(4-5), 427-442.
- Chiu, H.Y. (2014), *Beaufort wind scale*, Hong Kong Observatory, Hong Kong (http://www.weather.gov.hk/education/edu01met/wxobs/ele_beaufort2_e.htm).
- Cunha, A., Caetano, E. and Delgado, R. (2001), "Dynamic tests on large cable-stayed bridge", *J. Bridge Eng. - ASCE*, **6**(1), 54-62.
- Gade, S., Møller, N.B., Herlufsen, H. and Konstantin-Hansen, H. (2005), "Frequency domain techniques for operational modal analysis", *Proceedings of the 1st International Operational Modal Analysis Conference*, edited by R. Brincker and N. Møller, Copenhagen, Denmark.
- Hong Kong Observatory (2000), *Tropical cyclones in 1999*, Report, Hong Kong Observatory, Hong Kong.
- Ibrahim, S.R. (1977), "Random decrement technique for modal identification of structures", *J. Spacecraft Rockets*, **14**(11), 696-700.
- Jacobsen, N.J., Andersen, P. and Brincker, R. (2006), "Using enhanced frequency domain decomposition as a robust technique to harmonic excitation in operational modal analysis", *Proceedings of the ISMA Conference on Advanced Acoustics and Vibration Engineering*, Leuven, Belgium.
- James III, G.H., Carne, T.G. and Lauffer, J.P. (1995), "The natural excitation technique (NExT) for modal parameter extraction from operating wind turbines", *Int. J. Anal. Exper. Modal Anal.*, **10**(4), 260-277.
- Juang, J.N. and Pappa, R.S. (1985), "An eigensystem realization algorithm for modal parameter identification and model reduction", *J. Guid. Control Dynam.*, **8**(5), 620-627.
- Ko, J.M. and Ni, Y.Q. (2005), "Technology developments in structural health monitoring of large-scale bridges", *Eng. Struct.*, **27**(12), 1715-1725.
- Ko, J.M., Sun, Z.G. and Ni, Y.Q. (2002), "Multi-stage identification scheme for detecting damage in cable-stayed Kap Shui Mun Bridge", *Eng. Struct.*, **24**(7), 857-868.
- Liu, Y.C., Loh, C.H. and Ni, Y.Q. (2013), "Stochastic subspace identification for output-only modal analysis: application to super high-rise tower under abnormal loading condition", *Earthq. Eng. Struct. D.*, **42**(4), 477-498.
- Loh, C.H., Liu, Y.C. and Ni, Y.Q. (2012), "SSA-based stochastic subspace identification of structures from output-only vibration measurements", *Smart Struct. Syst.*, **10**(4-5), 331-351.
- Magalhães, F., Caetano, E. and Cunha, A. (2007), "Challenges in the application of stochastic modal identification methods to a cable-stayed bridge", *J. Bridge Eng. - ASCE*, **12**(6), 746-754.
- Magalhães, F., Cunha, A. and Caetano, E. (2008), "Dynamic monitoring of a long span arch bridge", *Eng. Struct.*, **30**(11), 3034-3044.
- Nayeri, R.D., Tasbihgoo, F., Wahbeh, M., Caffrey, J.P., Masri, S.F., Conte, J.P. and Elgamal, A. (2009), "Study of time-domain techniques for modal parameter identification of a long suspension bridge with dense sensor arrays", *J. Eng. Mech. - ASCE*, **135**(7), 669-683.
- Ni, Y.Q., Wong, K.Y. and Xia, Y. (2011), "Health checks through landmark bridges to sky-high structures", *Adv. Struct. Eng.*, **14**(1), 103-119.
- Peeters, B. and De Roeck, G. (1999), "Reference-based stochastic subspace identification for output-only modal analysis", *Mech. Syst. Signal Pr.*, **13**(6), 855-878.
- Peeters, B. and De Roeck, G. (2001), "Stochastic system identification for operational modal analysis: a review", *J. Dynam. Syst. Measurement Control*, **123**(4), 659-667.
- Peterson, L.D. (1995), "Efficient computation of the eigensystem realization algorithm", *J. Guid. Control, Dynam.*, **18**(3), 395-403.
- Pi, Y.L. and Mickleborough, N.C. (1989), "Modal identification of vibrating structures using ARMA model", *J. Eng. Mech. - ASCE*, **115**(10), 2232-2250.
- Siringoringo, D.M. and Fujino, Y. (2008), "System identification of suspension bridge from ambient vibration response", *Eng. Struct.*, **30**(2), 462-477.

- Van Overschee, P. and De Moor, B. (1993), "Subspace algorithms for the stochastic identification problem", *Automatica*, **29**(3), 649-660.
- Vandiver, J.K., Dunwoody, A.B., Campbell, R.B. and Cook, M.F. (1982), "A mathematical basis for the random decrement vibration signature analysis technique", *J. Mech. Design*, **104**(2), 307-313.
- Weng, J.H., Loh, C.H., Lynch, J.P., Lu, K.C., Lin, P.Y. and Wang, Y. (2008), "Output-only modal identification of a cable-stayed bridge using wireless monitoring systems", *Eng. Struct.*, **30**(7), 1820-1830.
- Wong, K.Y. (2004), "Instrumentation and health monitoring of cable-supported bridges", *Struct. Control Health Monit.*, **11**(2), 91-124.
- Wong, K.Y. (2007), "Design of a structural health monitoring system for long-span bridges", *Struct. Infrastruct. E.*, **3**(2), 169-185.